Nonlinear Analysis of Radial Evolution of Solar Wind in the Inner Heliosphere

**K. Kiran[1] · K.C. Ajithprasad[1] ·
V.M. Ananda Kumar[1] ⓘ · K.P. Harikrishnan[2]**

Abstract We analyzed the radial evolution of solar wind in the inner heliosphere using nonlinear time series tools such as correlation dimension D_2, correlation entropy K_2 and multifractal analysis, to get information regarding the inherent nonlinearity associated with the solar wind data and to know how it is affected by the radial distance from the Sun. Our study provides some detailed information regarding the change of dynamics of the fast solar wind with radial distance in the inner heliosphere, apart from confirming the previous observation about the chaotic nature in the dynamics of the slow solar wind. Also we found that the fast wind in the inner heliosphere is dominated by stochastic fluctuations. As the wind is flowing radially away from the Sun, stochastic fluctuation in the fast wind decreases. The stochastic fluctuation present in the data is a clear indication of the Alfvénic fluctuation associated with the solar wind. Finally, our analysis suggests that Alfvénic fluctuation strongly influences the solar wind as it flows radially outwards to mask the nonlinear component associated with the fast wind.

Keywords Solar wind · Waves, Alfvén · Turbulence

1. Introduction

The supersonic flow of charged particles from the hot corona of the Sun along with the magnetic field constitutes solar wind. This magnetized plasma can be classified into fast and slow

✉ K. Kiran
  kiranknair89@gmail.com

✉ K.C. Ajithprasad
  ajithprasadkc@gmail.com

✉ V.M. Ananda Kumar
  anandmgc@gmail.com

✉ K.P. Harikrishnan
  kp.hk05@gmail.com

[1] Department of Physics, M. G. College, Trivandrum 695604, India

[2] Department of Physics, Cochin College, Cochin 682002, India

wind based on their source of origin. The fast wind originates from open coronal holes that are uniform and stable. Its composition resembles that of the photosphere. The fast wind is Alfvén wave dominated (Ovenden, Shah, and Schwartz, 1983). Alfvén waves are transverse magnetohydrodynamic waves in which ions oscillate with magnetic tension on the magnetic field lines as the restoring force. Large-amplitude Alfvén waves propagating away from the Sun are considered to belong to the causes of coronal heating and acceleration of the solar wind (De Pontieu et al., 2007; Jess et al., 2009; McIntosh et al., 2011; Morton et al., 2012; Tomczyk et al., 2007). The slow wind originates from the lower solar latitude and is highly variable in terms of their speed, density, temperature, etc. Its composition resembles that of the corona (Schwenn, 1990). Alfvén waves in the fast wind evolve in the inner heliosphere getting weaker as the wind moves away from the Sun. Fast wind Alfvénicity becomes equal to that of slow wind near 0.3 AU. The slow wind turbulence is less Alfvénic compared to the fast wind and shows no radial dependence (Bruno and Carbone, 2013).

Systems in nature can be described either by linear or nonlinear models. Nonlinear models are generally more suitable for most real world systems (Kaplan and Glass, 1995). Thus nonlinear time series tools are essential to understand the dynamics of real world systems. Development of chaos theory and related techniques, applied to time series data, gives more potential to recover the underlying dynamics of the real world system from its complex temporal behavior (Abarbanel and Gollub, 1996; Ott, 2002; Abarbanel et al., 1993; Grassberger, Schreiber, and Schaffrath, 1991; Kugiumtzis, Lillekjendlie, and Christophersen, 1994; Lillekjendlie, Kugiumtzis, and Christophersen, 1994; Schuster, 1988; Kantz and Schreiber, 2004). Nonlinear time series analysis using chaos theory has been widely used in a variety of fields such as social science, astronomy, and physics (Schreiber, 1999). "Time delay embedding" is a method used in nonlinear time series analysis to reconstruct the phase space from single scalar time series data. In a dissipative system, time evolution trajectories in phase space converge to an invariant set called an attractor (Takens, 1981; Sauer, Yorke, and Casdagli, 1991). The static, as well as dynamic aspect of the attractors, are obtained by using certain nonlinear time series quantifiers such as correlation dimension, D_2, correlation entropy, K_2, and multifractal analysis, etc. (Mayer-Kress, 2012). A complexity measure which quantifies the geometry and shape of the attractor of a dynamical system is called the correlation dimension D_2. The variation of D_2 with embedding dimension M can be effectively used to characterize the measured time series data, since it is a measure of the dimension of the underlying attractor generated from the time series. For a random process, D_2 increase continuously with embedding dimension M, but for a chaotic process, D_2 saturates for some value of M. Correlation entropy K_2 represents the rate at which information is lost due to exponential divergence of trajectories in phase space in the case of a chaotic system (Ott, 2002). For a chaotic system, correlation entropy K_2 saturates as the embedding dimension M increases, but K_2 tends to zero as M tends to infinity for a random process. Multifractal analysis is an effective method to provide a statistical description of the strange attractors of a chaotic system.

Time series data available from the real world systems are affected by noise. A direct application of nonlinear techniques to the real world data may give spurious results if the noise component masks or dominates the inherent nonlinearity in the data. The effect of noise in the real world data can be effectively reduced by using nonlinear noise reduction techniques (Davies, 1994; Grassberger et al., 1993; Kantz et al., 1993; Kostelich and Schreiber, 1993; Schreiber, 1993).

The first step to begin the nonlinear time series analysis is hypothesis testing to confirm that the data are not resulting from a stochastic random process. Surrogate analysis is the method used for the hypothesis testing in the nonlinear time series analysis (Theiler

et al., 1992; Schreiber and Schmitz, 1996). The surrogate analysis also helps us to get an idea about the noise present in real world data (Harikrishnan et al., 2006). We use both D_2 and K_2 as a discriminating parameter (between noise and nonlinearity) in the surrogate analysis. The correlation entropy K_2 is more effective than the correlation dimension D_2 in the presence of colored noise which is correlated random process with the power varying with frequency as $1/(f^{\alpha})$ with the index α ranging from 1 to 2 (Kennel and Isabelle, 1992; Redaelli, Plewczyński, and Macek, 2002). The colored noise present in real world data gives a well saturated value of D_2, whereas pure white noise is scale free.

As solar wind dynamics contain information about coronal heating and solar wind acceleration, it is desirable to characterize these properties using time series analysis tools. The chaotic nature of the solar wind plasma is evident from the nonlinear time series analysis of slow speed solar wind, the interplanetary magnetic field, and the solar wind radio pulsation (Macek and Obojska, 1998, 1997; Macek and Redaelli, 2000; Pavlos et al., 1992; Polygiannakis and Moussas, 1994b,a). The multifractality of the solar wind chaotic attractor and change of the degree of multifractality as the wind evolves radially out from the Sun has also been studied using nonlinear time series tools (Macek, 2002, 2003, 2007; Marsch and Tu, 1994; Marsch, Tu, and Rosenbauer, 1996; Marsch and Tu, 1997; Carbone, 1993; Burlaga, 1991, 2001). The solar wind plasma studies are still relevant as many questions regarding solar wind plasma dynamics, radial evolution of the wind, the interaction of individual flow, etc., still remain unanswered. It is the turbulent nature of the solar wind plasma that demands the nonlinear time series tools for its analysis.

In the present study, we use an automated non-subjective algorithm scheme proposed by Harikrishnan et al. (2006), Harikrishnan, Misra, and Ambika (2009), Harikrishnan et al. (2009) for the computation of D_2, K_2 and the multifractal analysis. The method of computation is more useful for the comparison of the nonlinear measures computed from data and surrogates (as compared to methods based on TISEAN package). We use the TISEAN package to generate surrogate using Amplitude Adjusted Fourier Transformation (AAFT) procedure (Hegger, Kantz, and Schreiber, 1999; Hegger and Schreiber, 2002).

Our study mainly focuses on the radial dependence of the chaotic nature of the wind and how Alfvén waves influence the nonlinear and chaotic nature of the wind. We make a detailed nonlinear analysis of the radial evolution of the solar wind plasma in the inner heliosphere using our automated non-subjective algorithm scheme. Our algorithm allows us to compare the dynamics of solar wind plasma at different heliocentric distances in the presence of noise. It helps us to study the dynamics of solar wind plasma without using the nonlinear noise reduction methods. The nonlinear Alfvén waves in the solar wind are more dominant in the inner heliosphere. The Alfvén waves have a stochastic random nature (Ovenden, Shah, and Schwartz, 1983). The surrogate analysis provides an excellent qualitative estimate of noise in our data. It motivates us to study the change in the Alfvén wave in the solar wind as it radially flows out from the Sun.

Our paper is arranged as follows. Section 2 describes the data used for analysis. A detailed description of the methods used for the analysis of our data is given in Section 3. Results are presented in Section 4. Discussion and conclusion of our study are given in Section 5

2. Solar Wind Data

In the present study, we use radial component of velocity of solar wind plasma flow recorded in situ by Helios 2 at three different distances 0.3 AU, 0.7 AU and 0.9 AU during its primary

Figure 1 Plot of the slow (left panel) and the fast (right panel) solar wind measured at different radial distance from the Sun.
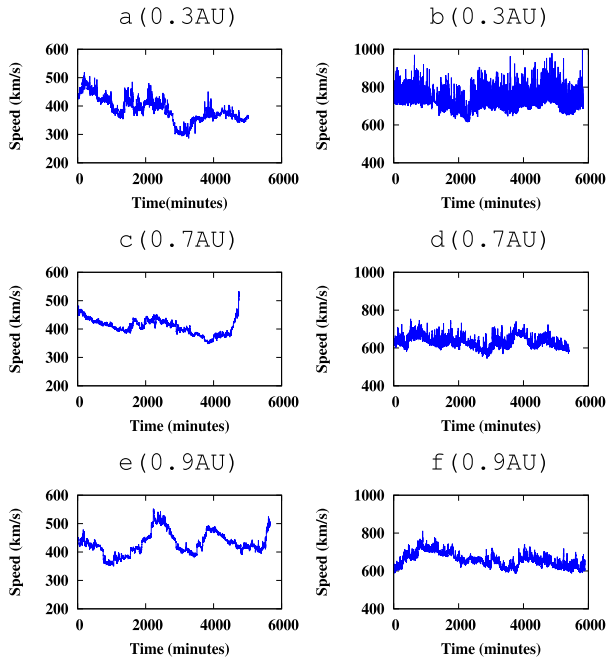
Table 1 Details of solar wind data used in our analysis.

Type	Radial distance from Sun (AU)	Date and time (dd:mm:yy:hh)
Slow	0.9	14:02:76:12–17:02:76:12
	0.7	12:03:76:00–14:03:76:12
	0.3	08:04:76:12–11:04:76:12
Fast	0.9	17:02:76:12–20:02:76:12
	0.7	15:03:76:12–18:03:76:12
	0.3	15:04:76:12–17:04:76:12

mission to the Sun. The observed data at three different distances are from the same co-rotating stream during three consecutive solar rotation. We divide the selected data at each heliospheric distances into two data sets; one continuous fast wind data set and another continuous slow wind data set. Each data set includes near about 6000 data points and the time interval between each data point is $\Delta t = 40.5$ s. The solar wind plasma used in our analysis is presented in Figure 1. Table 1 gives the heliocentric distances and the periods of different solar wind streams used in our analysis.

3. Nonlinear Measures Used for the Analysis

The Takens delay embedding method is used to reconstruct the entire phase space of the system from a single scalar time series output of the system. A multi-dimensional embedding space is created from the scalar time series $s(t_i)$ by choosing a suitable value of embedding

dimension M and delay time τ (Takens, 1981; Sauer, Yorke, and Casdagli, 1991)

$$X_n = \left[s(t_i), s(t_i + \tau), \ldots \ldots, s\big(t_i + (M-1)\tau\big) \right]. \tag{1}$$

The attractor in phase space is characterized by computing the correlation dimension D_2, the correlation entropy K_2 and the multifractal spectrum. Grassberger and Procaccia (1983a,b, 1984) used the time delay embedding method in the algorithm proposed for the computation of D_2 and K_2. In the present study, we use an automated modified Grassberger and Procaccia (GP) algorithm.

3.1. Correlation Dimension D_2

The correlation dimension quantifies the static aspect of the underlying attractor, such as the geometry of the attractor. Correlation dimension D_2 is defined as

$$D_2 = \lim_{R \to 0} \frac{d \log C_M(R)}{d \log R}. \tag{2}$$

Here $C_M(R)$ is the correlation sum. It is calculated as finding the relative number of data points within a distance R from a particular ith data point, say $p_i(R)$ in phase space,

$$p_i(R) = \lim_{N_v \to \infty} \frac{1}{N_v} \sum_{j=1, j \neq i}^{N_v} H\big(R - |\vec{x}_i - \vec{x}_j|\big), \tag{3}$$

where N_v is the total number of reconstructed vectors and H is the Heaviside step function. Averaging this quantity over randomly selected centers N_c gives the correlation sum

$$C_M(R) = \frac{1}{N_c} \sum_{i=1}^{N_c} p_i(R). \tag{4}$$

The correlation dimension measures how the correlation sum scales with distance in the embedded space.

3.2. Correlation Entropy K_2

Correlation entropy is the dynamic measure of the underlying attractor. It represents the rate at which the information is created when trajectories evolve in phase space (Ott, 2002). The relation connecting correlation entropy K_2 and correlation sum $C_M(R)$ is

$$K_2 \Delta t = \lim_{R \to 0} \lim_{M \to \infty} \lim_{N \to \infty} \log\left(\frac{C_M(R)}{C_{M+1}(R)} \right). \tag{5}$$

Here Δt is the time step between successive values in the time series.

In our modified scheme, we use a non-subjective algorithm approach for identifying the scaling region in the correlation sum for the computation of the correlation entropy K_2 and the correlation dimension D_2. The modified Grassberger and Procaccia (GP) algorithm computes several D_2 and K_2 for different values of R in the scaling region for a fixed M value and taking an average of these values. The error in D_2 and K_2 is the mean of the standard deviation of each value from this average value. The detailed algorithm is given in the papers of Harikrishnan, Misra, and Ambika (2009) and Harikrishnan et al. (2006).

3.3. Multifractal Spectrum

Chaotic dynamical systems always have strange attractors. The multifractal formalism is critical in determining the strange attractors present in dynamical systems and also providing a new statistical description to these sets. Strange attractors formed in the phase space due to the stretching and folding of trajectories have multifractal structure. Strange attractors always have a spectrum of dimension D_q, where the index q varies from $-\infty$ to $+\infty$ (Hentschel and Procaccia, 1983).

Since the dimension represents a scaling index, the spectrum of dimension implies that the chaotic attractor, in general, involves a range of scaling indices. In other words, different parts of the attractor scales differently. This spectrum of scaling indices is represented by what is called a multifractal spectrum. To get a formal definition of this, we divide the attractor into M dimensional cube of side ϵ. Let N_j be the number of points in the jth cube and N_T be the number of points on the attractor; then $p_j(\epsilon) = \frac{N_j}{N_T}$, the probability for the jth box.

This $p_j(\epsilon)$ scale with ϵ is given by

$$p_j(\epsilon) \propto \epsilon^{\alpha_j}, \tag{6}$$

where α_j is the scaling index for the jth cube. The number of cubes $g(\alpha)d\alpha$ having scaling index in the range α and $\alpha + d\alpha$ also varies as

$$g(\alpha) \propto \epsilon^{-f(\alpha)}, \tag{7}$$

where $f(\alpha)$ represent fractal dimension with singularity strength α. The D_q to $f(\alpha)$ transformation is done by using the Legendre transformation (Atmanspacher, Scheingraber, and Wiedenmann, 1989).

The generalized correlation dimension D_q is defined as

$$D(q) = \lim_{R \to 0} \frac{d(\log C_M^q(R))}{d(\log(R))}, \tag{8}$$

where $C_M^q(R)$ is the generalized correlation sum and is given by

$$C_M^q(R) = \left[\frac{1}{N_c} \sum_i^{N_c} \left(\frac{1}{N_v} \sum_{j=1, j \neq i}^{N_v} H\left(R - |\vec{X}_i - \vec{X}_j|\right) \right)^{q-1} \right]^{\frac{1}{q-1}}. \tag{9}$$

The generalized correlation dimension is also obtained by using a non-subjective algorithm approach proposed by Harikrishnan et al. (2009). In this approach, an analytic form of the $f(\alpha)$ function is first assumed to be

$$f(\alpha) = A(\alpha - \alpha_{min})^{\gamma_1}(\alpha_{max} - \alpha)^{\gamma_2}, \tag{10}$$

where A, γ_1, γ_2, α_{max}, α_{min} are set of parameters used to characterize a particular $f(\alpha)$ curve. Here "α_{min}" and "α_{max}" represent the extreme values of "α" and "γ_1" and "γ_2" specify the slope of the profile at the extreme points.

The above function satisfies the following conditions which are characteristic of any typical $f(\alpha)$ curve:

i) It is a single valued function between α_{max} and α_{min}.

Figure 2 Plot of the reconstructed phase space for the slow (left panel) and the fast (right panel) solar wind.
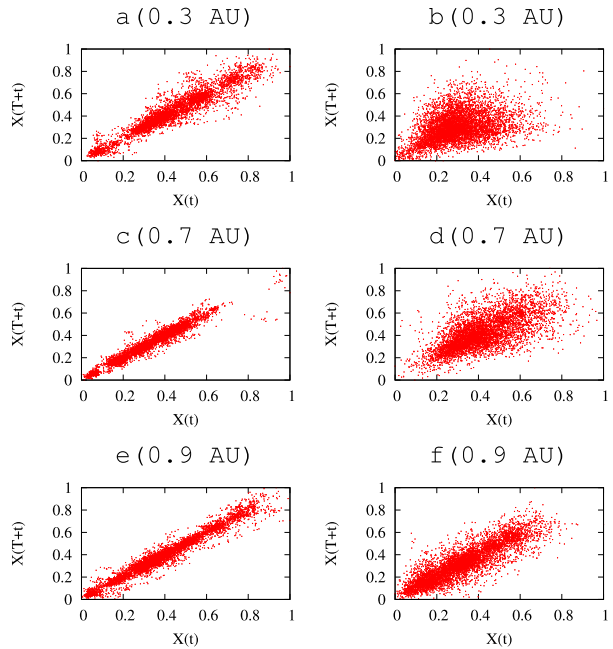
ii) It has a single maximum.

iii) $f(\alpha_{max}) = f(\alpha_{min}) = 0$.

iv) By imposing a condition on $f(\alpha)$ it can be shown that $0 < \gamma_1, \gamma_2 < 1$.

The important steps in the algorithm for the computation of $f(\alpha)$ are

i) First set the parameters $\alpha_{max} \cong D_{+\infty}$, $\alpha_{min} \cong D_{-\infty}$, $\alpha_1 \cong D_1$ and choose a value γ_1 in the range [0, 1].

ii) Use the input parameters and find the value of γ_2, A.

iii) Compute $f(\alpha)$ in the range α_{min} to α_{max}.

iv) Obtain D_q curve from $f(\alpha)$ using the inverse Legendre transformation.

v) Adjust the input parameters to obtain a D_q spectrum that best matches with D_q spectrum obtained from the time series.

vi) The final $f(\alpha)$ is obtained from the best fit D_q curve.

4. Results

Figure 2 presents the projection of attractor on to the two-dimensional subspace of the phase space for the fast and the slow solar wind at different radial distances from the Sun in the inner heliosphere. For the faithful comparison of the attractor, all the time series data are changed to a uniform deviate. Numerically, the time series is transformed into the range 0 to 1 which makes the embedding space unity. The attractor for the slow solar wind is shown in the left panel. The geometry of the attractor of the slow speed wind shows not much variation as the wind flows out from the Sun. The right panel shows the attractor for the fast wind in the inner heliosphere. The spread of attractor in phase space is greater for fast wind near 0.3 AU and 0.7 AU than the attractor near 0.9 AU. This result indicates that

Figure 3 Surrogate analysis of the slow (left panel) and the fast (right panel) solar wind using correlation dimension D_2 as discriminating parameter.
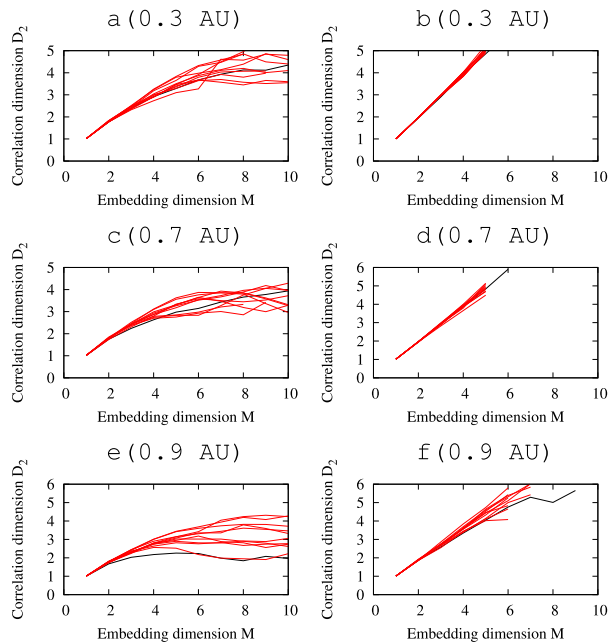

the percentage of white noise in the fast wind is higher in the inner heliosphere, and it is decreasing as the wind flows away from the Sun.

To determine the noise in the solar wind data in the inner heliosphere, we perform a surrogate analysis using the correlation dimension D_2 and the correlation entropy K_2 as discriminating parameters. The correlation entropy K_2 is a more effective discriminator in the presence of colored noise. In the present study, we made ten surrogates for each solar wind time series based on the AAFT procedure using the TISEAN code. Figure 3 presents the results of the surrogate analysis for all the solar wind with the correlation dimension D_2 as a discriminating measure. The fast wind near 0.3 AU and 0.7 AU shows a stochastic random behavior whereas the fast wind near 0.9 AU shows a slight deviation from its stochastic nature. A saturated value of correlation dimension D_2 is obtained for the slow solar wind and its surrogates. It indicates the presence of colored noise in the slow solar wind. The results of the surrogate analysis using the correlation entropy K_2 as a discriminating parameter are shown in Figure 4. The result obtained in the second surrogate analysis test also supports the results obtained in the first method. The colored noise contamination is more evident in the second method.

We calculated the correlation dimension D_2 of the solar wind flow, and the results are shown in Figure 5. The value of the correlation dimension D_2 of the slow solar wind is decreasing as it flows away from the Sun. Based on the above result, this change in D_2 value does not indicate any change in dynamics but confirms that white noise in the data decreases with distance from the Sun. This result also supports the presence of colored noise in the data. In the case of the fast wind, the presence of white noise is more dominant and behaves as a stochastic random process. However, near 0.9 AU the fast solar wind shows evidence of D_2 saturation with M. It indicates that the percentage of the white noise in the fast wind is more near the Sun and its percentage is slowly decreasing with distance from the Sun.

Figure 4 Surrogate analysis of slow (left panel) and fast (right panel) solar wind using correlation entropy K_2 as a discriminating parameter.
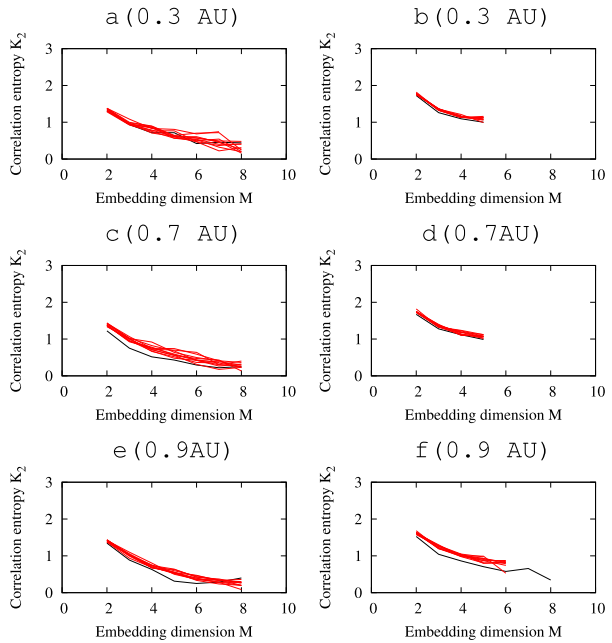

Figure 5 Variation of the correlation dimension D_2 with the embedding dimension M for the slow (left panel) and the fast (right panel) solar wind.
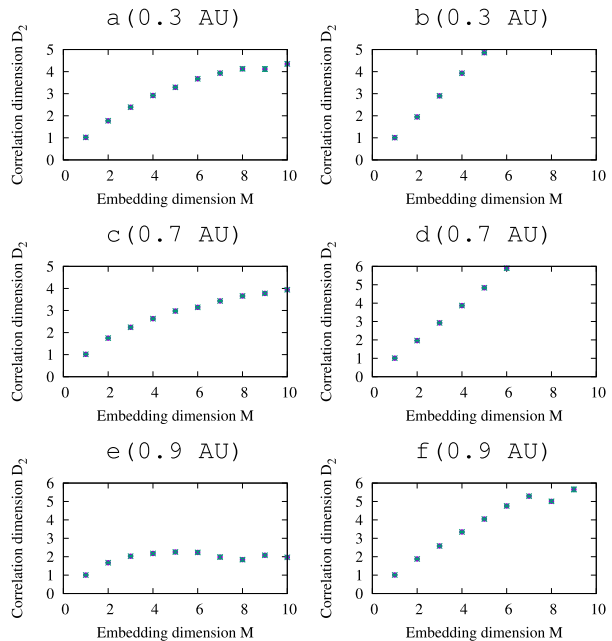
The results of the computation of the correlation entropy K_2 for different types of solar wind flow are shown in Figure 6. The results also suggest that slow wind in the inner helio-sphere does not show any dynamical modulation with distance from the Sun. The results of the correlation entropy K_2 for the fast wind also support its stochastic random nature.

Figure 6 Variation of the correlation entropy K_2 with the embedding dimension M for the slow (left panel) and the fast (right panel) solar wind. Several K_2 values are computed for different values of R in the scaling region for a fixed M value and an average of these values are taken. The error in K_2 is the mean of the standard deviation of each value from this average value.
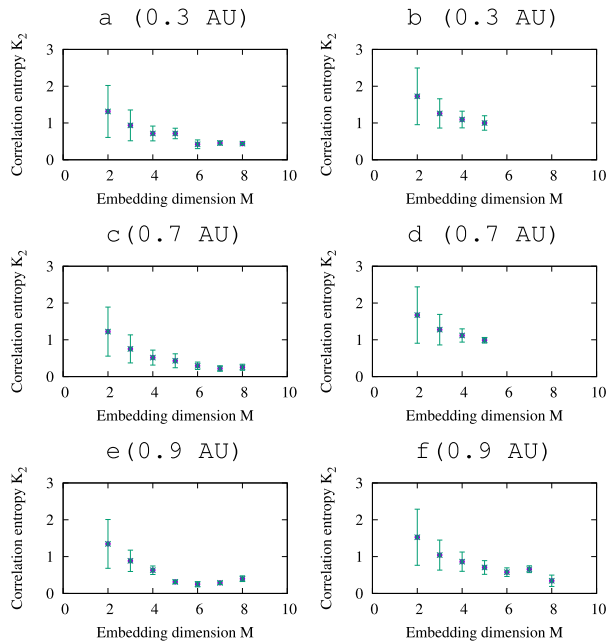

Finally, we show results of the multifractal analysis of both the slow and the fast wind in the inner heliosphere. The spectrum of dimension D_q of the strange attractors as a function of q for the fast and the slow wind are shown in Figure 7. The D_q versus q curve for the fast wind becomes steeper as the wind move away from the Sun, whereas the steepness of the curve for the slow wind shows no significant variation as the wind moves away from the Sun. Therefore one can say that both the slow and the fast wind in the inner heliosphere are the multifractal. The degree of multifractality of the fast wind increases with an increase in radial distance from the Sun and the degree of multifractality of the slow wind does not vary with radial distance from the Sun. The $f(\alpha)$ spectrum computed from the best fit D_q curve for both slow and fast wind are shown in Figure 8. The width of the $f(\alpha)$ spectrum for the fast wind increases as the wind moves away from the Sun, whereas the width for the slow wind show no significant variation. These observations also support the previous result. The narrow width of $f(\alpha)$ spectrum for the fast wind in the inner heliosphere supports white noise dominance in the wind because as the white noise in the data increase then the $f(\alpha)$ spectrum tends more and more towards a delta function.

5. Discussion and Conclusion

Nonlinear studies of the radial evolution of the solar wind provide a deeper understanding of the solar wind dynamics. The solar wind is a complex real world system. Its complex dynamics and evolution can be obtained from the comparison of nonlinear analysis results of the solar wind plasma at different radial distances from the Sun in the inner heliosphere. Our results confirm the deterministic chaotic nature of slow solar wind plasma as found in the previous studies. The previous studies have analyzed a change of dynamic of slow solar wind in the inner heliosphere using methods such as false nearest neighbors, average mutual

Figure 7 The spectrum of generalized dimension for the slow (left panel) and the fast (right panel) solar wind.
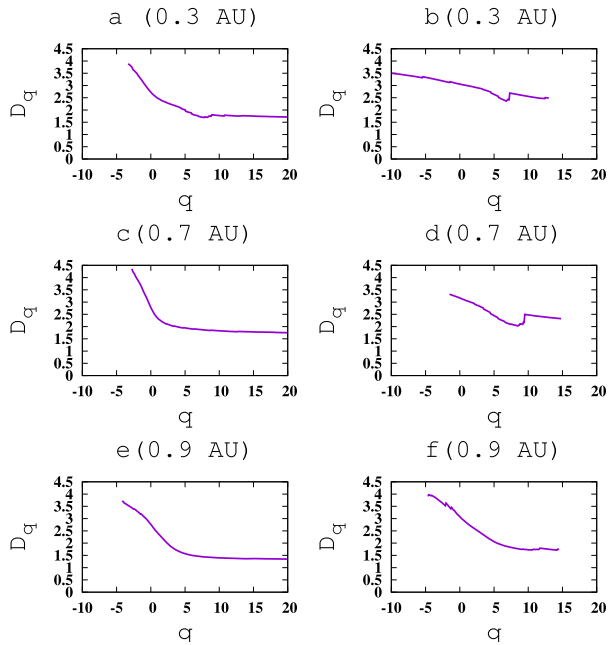
Figure 8 The $f(\alpha)$ spectrum for the slow (left panel) and the fast (right panel) solar wind.
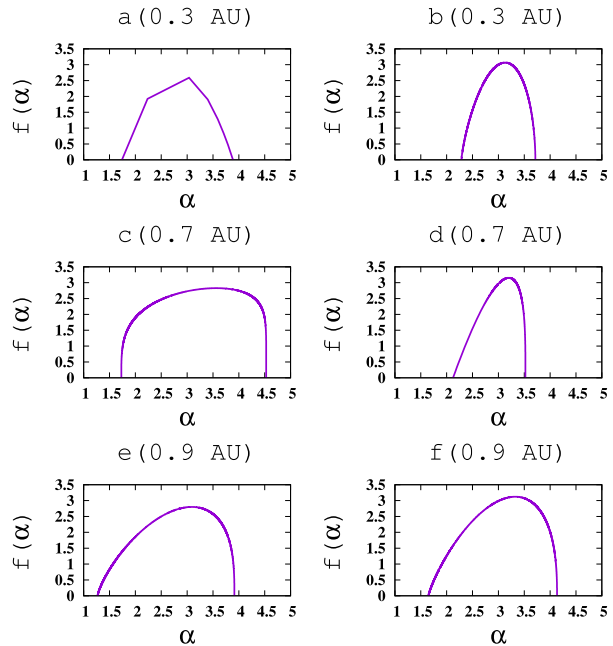
information, etc. But in the present study, we analyzed this problem in a detailed manner using correlation dimension D_2, correlation entropy K_2, surrogate analysis and multifractal analysis and obtained the same as previous result. Our results also give a good qualitaive

estimate of noise present in the slow solar wind in the inner heliosphere. Our results show that white noise and colored noise are present in the slow solar wind near the Sun and the colored noise become more and more dominant noise with an increase in distance from the Sun. The fast wind dynamics change in the inner heliosphere contrary to the slow solar wind. Our present study also analyzed these results in detail. We found that the fast wind in the inner heliosphere is a stochastic random process and a deviation from this stochastic character is found near 0.9 AU. The multifractal analysis done in our study clearly shows a dynamic change of the fast wind in the inner heliosphere. Also, we found that dominant noise present in the fast wind is white noise which decreases with an increase in radial distance from the Sun. The white noise masks the actual dynamics of the fast wind in the inner heliosphere.

Surrogate analysis in the present study strongly provides the following observation. White noise is present in both the fast and the slow wind. The presence of white noise is greater in the fast wind than in the slow wind. The white noise in both fast and slow wind decreases with increasing radial distance from the Sun, and this radial variation is more evident in the fast wind. The Alfvénic fluctuations in the solar wind have stochastic nature. Thus, we interpret stochastic random element in the solar wind as outward propagating Alfvén waves. The incompressive nature of Alfvénic fluctuations inhibits damping and leads to it dominating solar wind turbulence. The Alfvénic fluctuations are more dominant in the fast wind than in the slow wind. These Alfvénic fluctuations fade with increasing heliocentric distance. Our results indicate that the complex dynamics of the solar wind are characterized by a nonlinear process occurring at the source of origin and is convected along with the wind. The presence of large-amplitude Alfvén waves in the wind increases the stochastic nature of wind.

Based on the nonlinear analysis of the slow solar wind near 0.3 AU, the interplanetary magnetic field and the temperature near 1 AU, and radio pulsation have been confirming that the solar wind generates by some nonlinear process in the corona (Macek and Obojska, 1997, 1998; Macek and Redaelli, 2000; Pavlos et al., 1992; Polygiannakis and Moussas, 1994b,a; Kurths and Herzel, 1987). Hydrodynamic turbulence and intermittency characteristics of the solar wind plasma in the inner heliosphere have been obtained from previous work based on the multifractal analysis of solar wind data (Macek, 2002, 2003; Marsch and Tu, 1994; Marsch, Tu, and Rosenbauer, 1996; Marsch and Tu, 1997). These pieces of knowledge are still not enough to unveil the nature of solar wind that pervades the interplanetary space.

The results obtained in our work are in good agreement with the previous studies. Our results could be relevant in the sense that the radial evolution of the solar wind is very much related to Alfvén waves in the wind. The Alfvén wave-dominated fast wind is a stochastic random process and the less Alfvénic slow wind is chaotic. Our results set two important questions; the first is whether the Alfvén wave dominance in the fast wind masks the actual dynamics of the fast wind and the second is whether the different dynamics of both slow and fast wind is due to the source of origin or due to the Alfvén wave influence. To answer these questions, we need a detailed future study about solar wind plasma in the inner heliosphere and outer heliosphere. The future studies based on the data available from new missions like Parker Solar Probe and Solar Orbiter will provide a better idea about the solar wind source because these missions approach more closely to the Sun than Helios mission. These two missions will give more information regarding the source and evolution of slow solar wind. The information about Alfvénic slow wind closer to the Sun will be provided by Parker Solar Probe and, more about the source of solar wind plasma will be provided by Solar Orbiter.

Disclosure of Potential Conflicts of Interest   The authors declare that there are no conflicts of interest.

Publisher's Note   Springer Nature remains neutral with regard to jurisdictional claims in published maps and institutional affiliations.

References

Abarbanel, H., Gollub, J.: 1996, Analysis of observed chaotic data. *Phys. Today* **49**(11), 81.

Abarbanel, H.D., Brown, R., Sidorowich, J.J., Tsimring, L.S.: 1993, The analysis of observed chaotic data in physical systems. *Rev. Mod. Phys.* **65**(4), 1331.

Atmanspacher, H., Scheingraber, H., Wiedenmann, G.: 1989, Determination of $f(\alpha)$ for a limited random point set. *Phys. Rev. A* **40**(7), 3954.

Bruno, R., Carbone, V.: 2013, The solar wind as a turbulence laboratory. *Living Rev. Solar Phys.* **10**(1), 2.

Burlaga, L.: 1991, Multifractal structure of the interplanetary magnetic field: Voyager 2 observations near 25 AU, 1987–1988. *Geophys. Res. Lett.* **18**(1), 69.

Burlaga, L.: 2001, Lognormal and multifractal distributions of the heliospheric magnetic field. *J. Geophys. Res.* **106**(A8), 15917.

Carbone, V.: 1993, Cascade model for intermittency in fully developed magnetohydrodynamic turbulence. *Phys. Rev. Lett.* **71**(10), 1546.

Davies, M.: 1994, Noise reduction schemes for chaotic time series. *Physica D* **79**(2–4), 174.

De Pontieu, B., McIntosh, S., Carlsson, M., Hansteen, V., Tarbell, T., Schrijver, C., Shine, R., Tsuneta, S., Katsukawa, Y., Ichimoto, K., et al.: 2007, Chromospheric Alfvénic waves strong enough to power the solar wind. *Science* **318**(5856), 1574.

Grassberger, P., Procaccia, I.: 1983a, Characterization of strange attractors. *Phys. Rev. Lett.* **50**(5), 346.

Grassberger, P., Procaccia, I.: 1983b, Measuring the strangeness of strange attractors. *Physica D* **9**(1–2), 189.

Grassberger, P., Procaccia, I.: 1984, Dimensions and entropies of strange attractors from a fluctuating dynamics approach. *Physica D* **13**(1–2), 34.

Grassberger, P., Schreiber, T., Schaffrath, C.: 1991, Nonlinear time sequence analysis. *Int. J. Bifurc. Chaos* **1**(03), 521.

Grassberger, P., Hegger, R., Kantz, H., Schaffrath, C., Schreiber, T.: 1993, On noise reduction methods for chaotic data. *Chaos* **3**(2), 127.

Harikrishnan, K., Misra, R., Ambika, G.: 2009, Combined use of correlation dimension and entropy as discriminating measures for time series analysis. *Commun. Nonlinear Sci. Numer. Simul.* **14**(9–10), 3608.

Harikrishnan, K., Misra, R., Ambika, G., Kembhavi, A.: 2006, A non-subjective approach to the GP algorithm for analysing noisy time series. *Physica D* **215**(2), 137.

Harikrishnan, K., Misra, R., Ambika, G., Amritkar, R.: 2009, Computing the multifractal spectrum from time series: An algorithmic approach. *Chaos* **19**(4), 043129.

Hegger, R., Kantz, H., Schreiber, T.: 1999, Practical implementation of nonlinear time series methods: The TISEAN package. *Chaos* **9**(2), 413.

Hegger, R., Schreiber, T.: 2002, *The TISEAN software package*.

Hentschel, H., Procaccia, I.: 1983, The infinite number of generalized dimensions of fractals and strange attractors. *Physica D* **8**(3), 435.

Jess, D.B., Mathioudakis, M., Erdélyi, R., Crockett, P.J., Keenan, F.P., Christian, D.J.: 2009, Alfvén waves in the lower solar atmosphere. *Science* **323**(5921), 1582.

Kantz, H., Schreiber, T.: 2004, *Nonlinear Time Series Analysis* **7**, Cambridge University Press, Cambridge.

Kantz, H., Schreiber, T., Hoffmann, I., Buzug, T., Pfister, G., Flepp, L.G., Simonet, J., Badii, R., Brun, E.: 1993, Nonlinear noise reduction: A case study on experimental data. *Phys. Rev. E* **48**(2), 1529.

Kaplan, D., Glass, L.: 1995, Time-series analysis. In: *Understanding Nonlinear Dynamics*, Springer, New York, 278.

Kennel, M.B., Isabelle, S.: 1992, Method to distinguish possible chaos from colored noise and to determine embedding parameters. *Phys. Rev. A* **46**(6), 3111.

Kostelich, E.J., Schreiber, T.: 1993, Noise reduction in chaotic time-series data: A survey of common methods. *Phys. Rev. E* **48**(3), 1752.

Kugiumtzis, D., Lillekjendlie, B., Christophersen, N.D.: 1994, Chaotic time series: Part 1: Estimation of some invariant properties in state space. *Model. Identif. Control* **15**(4), 205.

Kurths, J., Herzel, H.: 1987, An attractor in a solar time series. *Physica D* **25**(1–3), 165.

Lillekjendlie, B., Kugiumtzis, D., Christophersen, N.: 1994, Chaotic time series part II: System identification and prediction. *arXiv preprint*. arXiv.

Macek, W.M.: 2002, Multifractality and chaos in the solar wind. In: *AIP Conference Proceedings* **622**, 74.

Macek, W.M.: 2003, The multifractal spectrum for the solar wind flow. In: *AIP Conference Proceedings* **679**, 530.

Macek, W.M.: 2007, Multifractality and intermittency in the solar wind. *Nonlinear Process. Geophys.* **14**(6), 695.

Macek, W.M., Obojska, L.: 1997, Fractal analysis of the solar wind flow in the inner heliosphere. *Chaos Solitons Fractals* **8**(10), 1601.

Macek, W.M., Obojska, L.: 1998, Testing for nonlinearity in the solar wind flow. *Chaos Solitons Fractals* **9**(1–2), 221.

Macek, W.M., Redaelli, S.: 2000, Estimation of the entropy of the solar wind flow. *Phys. Rev. E* **62**(5), 6496.

Marsch, E., Tu, C.: 1994, Non-Gaussian probability distributions of solar wind fluctuations. *Ann. Geophys.* **12**, 1127.

Marsch, E., Tu, C.-Y.: 1997, Intermittency, non-Gaussian statistics and fractal scaling of MHD fluctuations in the solar wind. *Nonlinear Process. Geophys.* **4**(2), 101.

Marsch, E., Tu, C.-Y., Rosenbauer, H.: 1996, Multifractal scaling of the kinetic energy flux in solar wind turbulence. *Ann. Geophys.* **14**, 259.

Mayer-Kress, G.: 2012, Dimensions and entropies in chaotic systems: quantification of complex behavior. In: *Proceeding of an International Workshop at the Pecos River Ranch, New Mexico, September 11–16, 1985* **32**, Springer, Berlin.

McIntosh, S.W., De Pontieu, B., Carlsson, M., Hansteen, V., Boerner, P., Goossens, M.: 2011, Alfvénic waves with sufficient energy to power the quiet solar corona and fast solar wind. *Nature* **475**(7357), 477.

Morton, R.J., Verth, G., Jess, D.B., Kuridze, D., Ruderman, M.S., Mathioudakis, M., Erdélyi, R.: 2012, Observations of ubiquitous compressive waves in the Sun's chromosphere. *Nat. Commun.* **3**(1), 1.

Ott, E.: 2002, *Chaos in Dynamical Systems*, Cambridge University Press, Cambridge.

Ovenden, C., Shah, H., Schwartz, S.: 1983, Alfvén solitons in the solar wind. *J. Geophys. Res.* **88**(A8), 6095.

Pavlos, G., Kyriakou, G., Rigas, A., Liatsis, P., Trochoutsos, P., Tsonis, A.: 1992, Evidence for strange attractor structures in space plasmas. *Ann. Geophys.* **10**, 309.

Polygiannakis, J., Moussas, X.: 1994a, Fractal properties of the interplanetary magnetic field fluctuations: indications of chaotic dynamics. *Astron. Astrophys.* **283**, 990.

Polygiannakis, J., Moussas, X.: 1994b, On experimental evidence of chaotic dynamics over short time scales in solar wind and cometary data using nonlinear prediction techniques. *Solar Phys.* **151**(2), 341.

Redaelli, S., Plewczyński, D., Macek, W.M.: 2002, Influence of colored noise on chaotic systems. *Phys. Rev. E* **66**(3), 035202.

Sauer, T., Yorke, J., Casdagli, M.: 1991, Embedology. *J. Stat. Phys.* **65**(3–4), 579.

Schreiber, T.: 1993, Extremely simple nonlinear noise-reduction method. *Phys. Rev. E* **47**(4), 2401.

Schreiber, T.: 1999, Interdisciplinary application of nonlinear time series methods. *Phys. Rep.* **308**(1), 1.

Schreiber, T., Schmitz, A.: 1996, Improved surrogate data for nonlinearity tests. *Phys. Rev. Lett.* **77**(4), 635.

Schuster, H.G.: 1988, *Deterministic chaos: An introduction*, 2nd revised edn. Verlagsgesellschaft mbH/VCH Publishers, Weinheim.

Schwenn, R.: 1990, Large-scale structure of the interplanetary medium. In: *Physics of the Inner Heliosphere I*, Springer, Berlin, 99.

Takens, F.: 1981, Detecting strange attractors in turbulence. In: *Dynamical Systems and Turbulence, Warwick 1980*, Springer, Berlin, 366.

Theiler, J., Eubank, S., Longtin, A., Galdrikian, B., Farmer, J.D.: 1992, Testing for nonlinearity in time series: The method of surrogate data. *Physica D* **58**(1–4), 77.

Tomczyk, S., McIntosh, S., Keil, S., Judge, P., Schad, T., Seeley, D., Edmondson, J.: 2007, Alfvén waves in the solar corona. *Science* **317**(5842), 1192.